

promoting access to White Rose research papers



Universities of Leeds, Sheffield and York
<http://eprints.whiterose.ac.uk/>

This is a copy of the final published version of a paper published via gold open access in **International Journal of Applied Glass Science**.

This open access article is distributed under the terms of the Creative Commons Attribution Licence (<http://creativecommons.org/licenses/by/3.0>), which permits unrestricted use, distribution, and reproduction in any medium, provided the original work is properly cited.

White Rose Research Online URL for this paper:
<http://eprints.whiterose.ac.uk/78579>

Published paper

Corkhill, CL, Cassingham, NJ, Heath, PG and Hyatt, NC (2013) Dissolution of UK high-level waste glass under simulated hyperalkaline conditions of a colocated geological disposal facility. *International Journal of Applied Glass Science*, 4 (4). 341 - 356. Doi: 10.1111/ijag.12042

Dissolution of UK High-Level Waste Glass Under Simulated Hyperalkaline Conditions of a Colocated Geological Disposal Facility

Claire L. Corkhill, Nathan J. Cassingham, Paul. G. Heath, and Neil C. Hyatt*

Immobilisation Science Laboratory, Department of Materials Science and Engineering, The University of Sheffield, Mappin Street, Sheffield S1 3JD, UK

We report analysis of chemical durability of UK HLW MW+25% simulant glass under model hyperalkaline conditions of a colocated geological disposal facility. Glass powders and monoliths were dissolved for 168 days in saturated $\text{Ca}(\text{OH})_2$. Dissolution in the presence of high concentrations of Ca (>200 mg/L) was an order of magnitude lower than dissolution in water. Dissolution of Si did not occur until a Ca:Si ratio of <2 was achieved. The mechanism of dissolution involved the incorporation of Ca into the hydrated surface (initial, incubation regime), the precipitation of C-S-H phases, including a range of compositions in the C-(N)-(A)-S-H and M-S-H systems (intermediate regime), and the precipitation of C-S-H phases (the residual regime). Thermodynamic analysis and consideration of the $\text{CaO-SiO}_2\text{-H}_2\text{O}$ phase diagram suggest that the rate-limiting step of glass dissolution in Ca-rich solutions is Ca-Si equilibrium, involving the precipitation of C-S-H phases, which change in chemical composition as a function of solution chemistry. In low SA/V ratio experiments, the dissolution progressed only to the initial incubation regime, resulting from fewer surface sites for Ca incorporation. Overall, these results suggest that Ca and Si in solution play an important role in the long-term durability of UK HLW in Ca-rich solutions.

Introduction

The current immobilization route for UK high-level waste (HLW) is vitrification within a borosilicate glass blend, comprising a mixture of Magnox reactor waste (25%) and thermal oxide reprocessing (ThORP) waste (75%). Vitrification of HLW is performed using

the AVH (Atelier de Vitrification de la Hague) process at the Sellafield site, United Kingdom, where it is stored for at least 50 years, awaiting final disposal. It is proposed that this waste will be disposed of in a deep geological disposal facility (GDF), comprising multiple layers of engineered protection, several hundreds of meters below the ground.¹ One of the suggested concepts for the future UK GDF is a colocated HLW and intermediate-level waste (ILW) geological repository.¹ In the HLW “zone,” vitrified waste in steel canisters will be placed within deposition holes in the bedrock and backfilled with bentonite clay, which provides a low-permeability barrier to water infiltration and radionuclide

*n.c.hyatt@sheffield.ac.uk

release. In the ILW “zone,” drums containing waste encapsulated in cement will be emplaced and backfilled with a cementitious grout.² Due to its high porosity and permeability, when water infiltrates the GDF, the cement grout will quickly become saturated with groundwater. As a result, $\text{Ca}(\text{OH})_2$ in the grout will dissolve creating high-pH conditions (pH 10–12), with the aim of limiting the solubility of radionuclide species and releasing high concentrations of Ca into the GDF groundwaters.³ Because the flow of this Ca-rich, hyperalkaline water from the ILW “zone” to the HLW “zone” of the colocated repository cannot be precluded, it is important to understand the dissolution behavior of HLW glass under conditions that simulate this colocated repository, using a simplified model system.

A number of studies have considered the effect of high pH on the early dissolution of simulant high-level waste glasses of varying composition. In general, dissolution rates are found to be pH dependent, with significantly higher dissolution rates observed above pH 9.^{4,5} It has been suggested that enhanced dissolution is likely due to a breakdown of the silicate network.⁶ These studies used hydroxides of sodium and potassium to buffer the pH to higher values, which are not expected to interact with dissolved glass components significantly during early stages of dissolution. Conversely, in the case of $\text{Ca}(\text{OH})_2$, it has been shown that Ca reacts with Si dissolved species, which may affect the dissolution mechanism and rate. Recent studies have assessed the dissolution of borosilicate glass in the presence of calcium-rich solutions.^{7–10} These authors observed the formation of a C-S-H gel on the surface of the glass and concluded that this “alteration layer” acted to passivate the dissolution of the glass. During the preparation of this manuscript, Mercardo-Depierre *et al.*¹¹ proposed that the durability of glass in saturated Ca solution was dependent on the silicon–calcium reactivity.

There is currently limited knowledge on the aqueous durability of UK HLW glass for use in the postclosure safety assessment of UK vitrified waste product, particularly in a colocated geological disposal concept. Furthermore, the focus of previous work has been on short time scales, typically <1 month.¹² UK HLW glasses have a higher Mg content than most other glasses developed internationally, which is known to have a significant effect on the dissolution rate and alteration products formed.¹³ The aim of this study was to develop an understanding of the dissolution of UK HLW glass (MW+25%) in a colocated HLW and ILW geological

disposal facility, using a model system. The effect of a high-pH, $\text{Ca}(\text{OH})_2$ -saturated solution at 50°C (the predicted temperature of the GDF several thousand years after closure) is investigated over a period of 168 days using powdered, semi-static dissolution experiments. For comparison, the UK HLW glass powder was also dissolved in initially pure water. To investigate the effect of surface-area-to-volume ratio on the dissolution of UK HLW glass in saturated $\text{Ca}(\text{OH})_2$, monolith dissolution experiments were also conducted, including a preliminary analysis of the alteration layer formed. The observed dissolution is described in terms of thermodynamic equilibrium between Ca and Si, using geochemical modeling.

Experimental Procedure

Glass Preparation

The glass used in this study was prepared as a nonradioactive analog for a UK HLW glass MW+25%. 75 wt% borosilicate glass frit was mixed with 25 wt% simulated HLW calcine supplied by The National Nuclear Laboratory, United Kingdom. After mixing, the frit and calcine were melted in a mullite crucible at 1060°C (1 h) and subsequently stirred (mullite stirrer, 4 h) prior to casting into a preheated stainless steel mould. Annealing was performed at 500°C (1 h), and the glass was allowed to cool at 1°C/min to room temperature. The glass composition, determined by X-ray fluorescence, is given in Table I.

Table I. Elemental composition of MW+25% HLW glass, as determined by XRF

Oxide	Wt%	Oxide	Wt%
SiO_2	45.77	MgO	1.33
B_2O_3	18.1	MoO_3	2.00
Na_2O	8.03	Nd_2O_3	1.79
Li_2O	4.76	NiO	0.28
Al_2O_3	1.85	Pr_2O_3	0.46
BaO	1.21	RuO_2	0.48
CeO_2	1.23	Sm_2O_3	0.28
Cr_2O_3	0.37	SrO	0.32
Cs_2O	1.59	TeO_2	0.28
Fe_2O_3	1.85	Y_2O_3	0.10
Gd_2O_3	3.82	ZrO_2	2.37
La_2O_3	0.66	Total	98.93

The glass was crushed, sieved to 35–53 μm , and cleaned according to the PCT-B ASTM standard.¹⁴ Glass monoliths were cut to dimensions of 10.5 \times 10.5 \times 4.5 mm (± 1 mm) for use in MCC-1 tests.¹⁵ These were ground (SiC paper) and polished (3 μm diamond paste) to 10.0 \times 10.0 \times 4.0 mm (± 0.1 mm) and subsequently cleaned by repeatedly rinsing and cleaning in an ultrasonic bath in high-purity H_2O and ethanol. Cleaned monoliths were dried at 90°C overnight.

Dissolution Experiments

Two solutions were prepared for the semi-static powder durability experiments: (i) nitrogen de-aerated (<1 ppm oxygen, measured using an electrochemical sensor), nonbuffered ultra-high-quality water (18 M Ω) solution; and (ii) nitrogen de-aerated (<1 ppm oxygen, as above), saturated $\text{Ca}(\text{OH})_2$ solution (made using ultra-high-quality water). Because the solubility of $\text{Ca}(\text{OH})_2$ decreases with increasing temperature, the saturated $\text{Ca}(\text{OH})_2$ solution used was prepared at the experimental temperature to minimize the precipitation of solid $\text{Ca}(\text{OH})_2$. The pH of the solution was measured as pH 12.4 (corrected to 25°C), indicating that full saturation had been achieved. It is important to note that pH measurements were not corrected for the high ionic strength of the solution; therefore, the pH values reported in $\text{Ca}(\text{OH})_2$ experiments are indicative, rather than absolute. All experiments were performed in a nitrogen-atmosphere glove box. Oxygen levels (as an assessment of any residual air content and thus indirectly CO_2 content, which may lead to the formation of calcium carbonate precipitates in solution) were measured to be less than 20 ppm.

400 mL of each solution was added to 500-mL HDPE vessels. In this volume, the surface-area-to-volume ratio for the powder was 10 000/m. This is a deviation from the standard PCT test, which recommends a surface-area-to-volume ratio of 2000/m.¹⁴ This increase was made to enable glass performance to be investigated in the residual rate regime, by rapidly saturating the solution in dissolved elements. The glass powder was added to the solution, and the vessels were sealed and placed in an oven within the glove box at 50°C. Experiments were conducted in triplicate, with duplicate blanks containing no glass. 5-mL aliquots of solution were taken at 1, 3, 7, 14, 21, 28, 42, 56, 70, 84, 112, 140, and 168 days. Aqueous elemental con-

centrations, including Ca (reported in mg/L), were determined using ICP-OES and ICP-MS (Sheffield Assay Office), and the pH was measured. Monoliths were placed on a Teflon cradle in Teflon reaction vessels containing saturated $\text{Ca}(\text{OH})_2$ and sampled as for the powder experiment. The surface-area-to-volume ratio was 10/m. The normalized mass loss of elements within the glass was calculated according to Eq. 1, where NL_i is the normalized mass loss (g/m^2) value of element i , c_i is the concentration (mg/L) of element i in the experimental solution, f_i is the mass fraction (wt%/100) of element i found in the glass, and SA/V is the ratio (/m) between the surface area of the glass and the volume of solution used. The surface-area-to-volume ratio was corrected for evaporative losses at each sampling point.

$$NL_i = \frac{c_i}{f_i \times (SA/V)} \quad (1)$$

The normalized dissolution rate, RL_i ($\text{g}/\text{m}^2/\text{day}$), was determined, according to Eq. 2, where t is the time in days:

$$RL_i = \frac{c_i}{f \times (SA/V) \times t} \quad (2)$$

Analysis of the experimental data was performed using the geochemical modeling software PHREEQC,¹⁶ using the LLNL (Lawrence Livermore National Laboratory) database. Aqueous elemental concentrations and pH data from the experimental solutions were modeled to determine relative saturation indices of potential equilibrium phases.

Post Dissolution Sample Analysis

The monolith glass sample was removed from the experimental solution after 168 days, rinsed with UHQ water, and left to dry for 24 h at room temperature. Imaging was conducted using scanning electron microscopy (SEM) (JEOL 6400) operating at an accelerating voltage of 15–20 keV and a working distance of 15.0 \pm 0.1 mm. The SEM was equipped with energy dispersive spectroscopy (EDS; Inca, Oxford, UK), which was used to perform line scans across the cross-sectioned monolith embedded in epoxy resin, in order to ascertain the final chemistry of any alteration layer formed. X-ray diffraction analysis was performed to identify any secondary phases on the surface of the monolith glass, as a

function of time, using a Siemens D5000 diffractometer with a Cu K α source; diffraction patterns were collected between $5 < 2\theta < 90^\circ$ at $2^\circ/\text{min}$.

Results

UK HLW glass powder dissolution in water

The average pH of the solution in contact with the simulant UK HLW glass powder was $\text{pH } 9.8 \pm 0.1$, compared with the blank pH of ~ 6.1 . These values were little changed over the duration of the experiment, indicating that the pH was quickly buffered to a stable value (Fig. 1a). The normalized mass loss of boron (NL_{B}) is shown in Fig. 1b. Boron is a well-recognized soluble tracer element for network dissolution and is thought not to become incorporated into alteration products during glass alteration; hence, it may be used as an indication of forward glass dissolution rate. NL_{B} data for all experimental conditions are shown in Table II. NL_{B} occurred under two main dissolution regimes: an initial rapid rate was observed between 0 and 28 days, followed by a slower rate from 28 days until the end of the experiment at 168 days. Similar dissolution trends were also observed for NL_{Li} (Fig. 1c) and NL_{Na} (Fig. 1d), although Na dissolution was greater than that for B and Li (Table II); however, this may be expected as a result of the alkali-rich nature of the glass (Table I). Dissolution rates are shown in Table III. In the course of the experiment, the curves did not reach a plateau value, indicating that equilibrium or, in the case of glass, “quasi-equilibrium” was not achieved.

The normalized mass loss of silicon, NL_{Si} , between 0 and 28 days was rapid (Fig. 1e), at a rate of $(3.32 \pm 0.3) \times 10^{-5} \text{ g/m}^2/\text{day}$ (Table III). This dissolution behavior was followed by a decrease in the dissolution rate to $(4.21 \pm 0.4) \times 10^{-7} \text{ g/m}^2/\text{day}$ until a steady state was achieved at NL_{Si} of $(9.94 \pm 0.9) \times 10^{-4} \text{ g/m}^2$. This is indicative of silicon saturation in solution, likely a result of the high surface-area-to-volume ratio of the glass powder employed in this study. The normalized mass loss of Mg and Al was significantly less than those observed for B, Li, Na, and Si (Figs 1g and h, respectively). The NL_{Mg} was measured at relatively high concentrations between 0 and 28 days with a maximum NL_{Mg} value of $(5.5 \pm 0.4) \times 10^{-5} \text{ g/m}^2$. Subsequently, the NL_{Mg} rapidly decreased to a constant value of $(5.9 \pm 1.1) \times 10^{-6} \text{ g/m}^2$ until the end of the experiment. The NL_{Al} was initially high, decreasing

from 0 to 7 days to an approximately constant value of $(8.8 \pm 0.2) \times 10^{-7} \text{ g/m}^2$. The dissolution behavior of both Mg and Al is indicative of incorporation into a gel layer on the surface of the glass powders.

UK HLW glass powder dissolution in saturated Ca(OH)₂

The pH of the saturated Ca(OH)_2 solution containing UK HLW glass powder decreased rapidly from an initial value of $\text{pH } 12.7 \pm 0.1$ to $\text{pH } 10.5 \pm 0.2$ at 84 days, where it remained constant, as shown in Fig. 1a. This is in comparison with the blank saturated Ca(OH)_2 solution, which had a constant pH of 12.5 ± 0.3 for the duration of the experiment (Fig. 1a). The pH of the solution was consistently higher than pH 11.5, indicating that Ca(OH)_2 precipitation from solution (due to carbonation) was minimized.

The normalized mass loss of B, Li, and Na is shown in Figs 1b–d. It is clear that the dissolution behavior of these elements in saturated Ca(OH)_2 was different to that observed in water. Firstly, lower $\text{NL}_{\text{(i)}}$ values and dissolution rates (Tables II and III) were observed, and secondly, the dissolution appeared to occur over three main dissolution regimes: from 0 to 28 days, 28 to 84 days, and 84 to 168 days. Tables II and III detail the $\text{NL}_{\text{(i)}}$ and $\text{RL}_{\text{(i)}}$ for each period, respectively. For B, the $\text{NL}_{\text{(i)}}$ was initially fast, with RL_{B} of $(5.92 \pm 0.6) \times 10^{-5} \text{ g/m}^2/\text{day}$ between 0 and 28 days. From 28 to 84 days, the dissolution rate decreased to $(2.91 \pm 0.3) \times 10^{-5} \text{ g/m}^2/\text{day}$ and decreased further from 84 to 168 days ($\text{RL}_{\text{B}} = (1.37 \pm 0.1) \times 10^{-5} \text{ g/m}^2/\text{day}$). The data suggest that “quasi-equilibrium” was achieved, but further data are required to confirm this.

The NL_{Si} is shown in Fig. 1e. Initially, Si was not detectable in solution. At 28 days, it was possible to measure Si, giving NL_{Si} of $(3.14 \pm 0.3) \times 10^{-5} \text{ g/m}^2$ (Table II). After this initial “incubation” regime, dissolution of silicon proceeded rapidly between 28 and 84 days. Between 84 and 168 days, the dissolution rate decreased to $(4.47 \pm 0.5) \times 10^{-6} \text{ g/m}^2/\text{day}$, where an apparently constant NL_{Si} of $(8.16 \pm 0.8) \times 10^{-4} \text{ g/m}^2$ was attained. This dissolution behavior is in contrast to that observed for glass powder dissolved in water, which demonstrated a rapid increase between 0 and 28 days followed by a constant NL_{Si} until the end of the experiment (Fig. 1e). These data suggest that the presence of Ca(OH)_2 in solution directly affected the NL_{Si} .

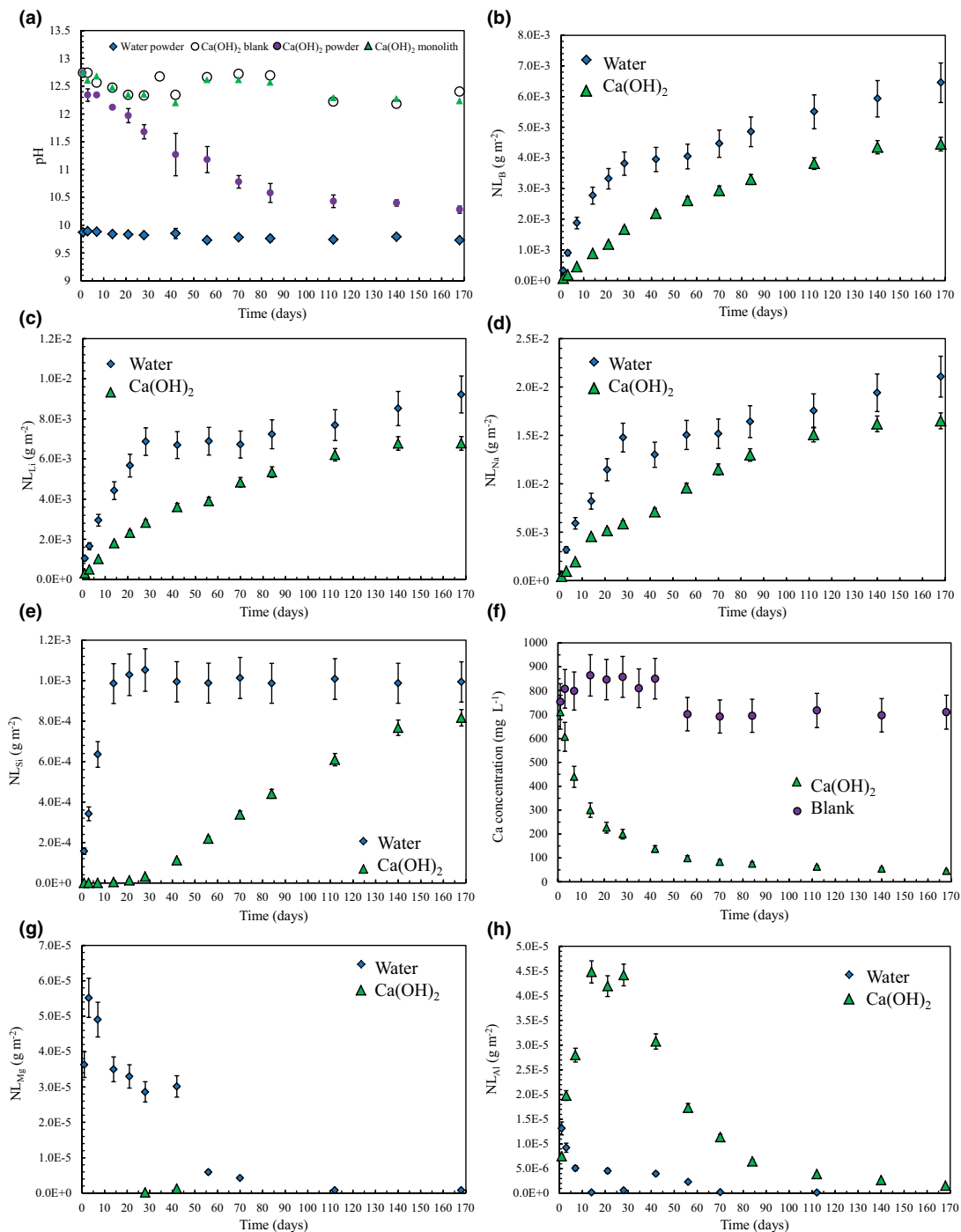


Fig. 1. (a) Measured solution pH for UK HLW glass powders and monoliths dissolved in water and/or saturated Ca(OH)_2 solution. Normalized mass loss (g m^{-2}) of: (b) B, (c) Li, (d) Na, and (e) Si from glass powder dissolved in water or Ca(OH)_2 ; (f) solution concentration (mg L^{-1}) of dissolved Ca in blank (i.e. no glass) saturated Ca(OH)_2 solution and for UK HLW glass powder; and normalized mass loss (g m^{-2}) of (g) Mg and (h) Al from glass powder dissolved in water or Ca(OH)_2 . Error bars are derived from standard deviation of triplicate samples.

Table II. Normalized mass loss (g/m^2) of B, Li, Na, and Si during the three main phases of dissolution in water and saturated $\text{Ca}(\text{OH})_2$ solution for all experimental conditions, described by the end time point of each regime

	B	NL _i (g/m^2) Li	Na	Si
Water (powder)				
28 days	$(3.81 \pm 0.3) \times 10^{-3}$	$(6.87 \pm 0.7) \times 10^{-3}$	$(1.48 \pm 0.1) \times 10^{-2}$	$(1.05 \pm 0.1) \times 10^{-3}$
168 days	$(6.45 \pm 0.6) \times 10^{-3}$	$(9.22 \pm 0.9) \times 10^{-3}$	$(2.11 \pm 0.2) \times 10^{-2}$	$(9.94 \pm 0.9) \times 10^{-4}$
Saturated $\text{Ca}(\text{OH})_2$				
<i>Powder</i>				
28 days	$(1.67 \pm 0.2) \times 10^{-3}$	$(2.83 \pm 0.2) \times 10^{-3}$	$(5.88 \pm 0.6) \times 10^{-3}$	$(3.14 \pm 0.3) \times 10^{-5}$
84 days	$(3.30 \pm 0.3) \times 10^{-3}$	$(5.35 \pm 0.5) \times 10^{-3}$	$(1.30 \pm 0.1) \times 10^{-2}$	$(4.41 \pm 0.4) \times 10^{-4}$
168 days	$(4.45 \pm 0.5) \times 10^{-3}$	$(6.78 \pm 0.6) \times 10^{-3}$	$(1.65 \pm 0.2) \times 10^{-2}$	$(8.16 \pm 0.8) \times 10^{-4}$
<i>Monolith</i>				
70 days	$(1.96 \pm 0.2) \times 10^{-2}$	$(2.67 \pm 0.3) \times 10^{-2}$	$(3.39 \pm 0.4) \times 10^{-2}$	(0.0 ± 0.0)
168 days	$(3.02 \pm 0.3) \times 10^{-2}$	$(4.40 \pm 0.4) \times 10^{-2}$	$(6.89 \pm 0.2) \times 10^{-2}$	(0.0 ± 0.0)

Table III. Normalized dissolution rates ($\text{g/m}^2/\text{day}$) of B, Li, Na, and Si during the three main regime of dissolution in water and saturated $\text{Ca}(\text{OH})_2$ solution for all experimental conditions

	B	RL _i ($\text{g/m}^2/\text{d}$) Li	Na	Si
Water (powder)				
Initial (0–28 days)	$(1.29 \pm 0.1) \times 10^{-4}$	$(2.16 \pm 0.2) \times 10^{-4}$	$(5.24 \pm 0.5) \times 10^{-4}$	$(3.32 \pm 0.3) \times 10^{-5}$
Residual (28–168 days)	$(1.88 \pm 0.2) \times 10^{-5}$	$(1.68 \pm 0.2) \times 10^{-5}$	$(4.49 \pm 0.5) \times 10^{-5}$	$(4.21 \pm 0.4) \times 10^{-7}$
Saturated $\text{Ca}(\text{OH})_2$				
<i>Powder</i>				
Initial (0–28 days)	$(5.92 \pm 0.6) \times 10^{-5}$	$(9.32 \pm 0.9) \times 10^{-5}$	$(2.02 \pm 0.4) \times 10^{-4}$	$(3.32 \pm 0.3) \times 10^{-7}$
Intermediate (28–84 days)	$(2.91 \pm 0.3) \times 10^{-5}$	$(4.50 \pm 0.5) \times 10^{-5}$	$(1.27 \pm 0.1) \times 10^{-4}$	$(7.31 \pm 0.7) \times 10^{-6}$
Residual (84–168 days)	$(1.37 \pm 0.1) \times 10^{-5}$	$(1.71 \pm 0.2) \times 10^{-5}$	$(4.19 \pm 0.4) \times 10^{-5}$	$(4.47 \pm 0.5) \times 10^{-6}$
<i>Monolith</i>				
Initial (0–70 days)	$(1.68 \pm 0.2) \times 10^{-4}$	$(3.53 \pm 0.4) \times 10^{-4}$	$(6.70 \pm 0.7) \times 10^{-4}$	(0.0 ± 0.0)
Intermediate (70–168 days)	$(5.44 \pm 0.7) \times 10^{-5}$	$(1.77 \pm 0.4) \times 10^{-4}$	$(3.57 \pm 0.4) \times 10^{-4}$	(0.0 ± 0.0)

The concentration of Ca remained approximately constant in the blank $\text{Ca}(\text{OH})_2$ solution at 770 ± 68 mg/L, as shown in Fig. 1f. Conversely, for the $\text{Ca}(\text{OH})_2$ solution in contact with UK HLW glass powder, the Ca concentration rapidly decreased from a starting value of 770 mg/L at 0 days to 200 mg/L at 28 days. Concentrations continued to decrease between 28 and 84 days at a much slower rate (to ~ 80 mg/L), and finally, after 84 days, a constant Ca concentration of

65 ± 10 mg/L was observed. These changes in Ca removal from solution are concurrent with the decrease in pH (Fig. 1a), which was also constant at 84 days and beyond. Figs 1g and h show the evolution of $\text{NL}_{(\text{Mg})}$ and $\text{NL}_{(\text{Al})}$, respectively. In contrast to the $\text{NL}_{(\text{Mg})}$ observed for UK HLW dissolved in water, it was not always possible to detect Mg in solution. The only detectable concentrations occurred at 28 and 42 days, giving $\text{NL}_{(\text{Mg})}$ of $\sim 10^{-7}$ m²/g. Interestingly, the $\text{NL}_{(\text{Al})}$ was observed to

rapidly increase in solution, reaching a maximum value of $(4.36 \pm 0.2) \times 10^{-5}$ g/m² between 14 and 28 days. After this time, the $NL_{(Al)}$ slowly decreased to a value of $(1.55 \pm 0.1) \times 10^{-6}$ g/m² at 168 days. This is in contrast to the behavior observed in water only, where the $NL_{(Al)}$ was constantly at low values.

Geochemical modeling of the experimental solution resulting from UK HLW glass powder dissolution in saturated $Ca(OH)_2$ was conducted using PHRE-

EQC. Saturation indices of phases shown to be typically relevant to glass dissolution at high pH^{4,17} and those containing Ca are shown in Fig. 2a, as a function of the three apparent regimes of dissolution. Also included were Si phases containing Al and Mg, as a result of the distinctive normalized mass loss of these elements (Figs. 1g-h). The phases investigated were the following: analcime ($Na_{0.96}Al_{0.96}Si_{2.04}O_6 \cdot H_2O$), which is known to precipitate during the dissolution of silicate

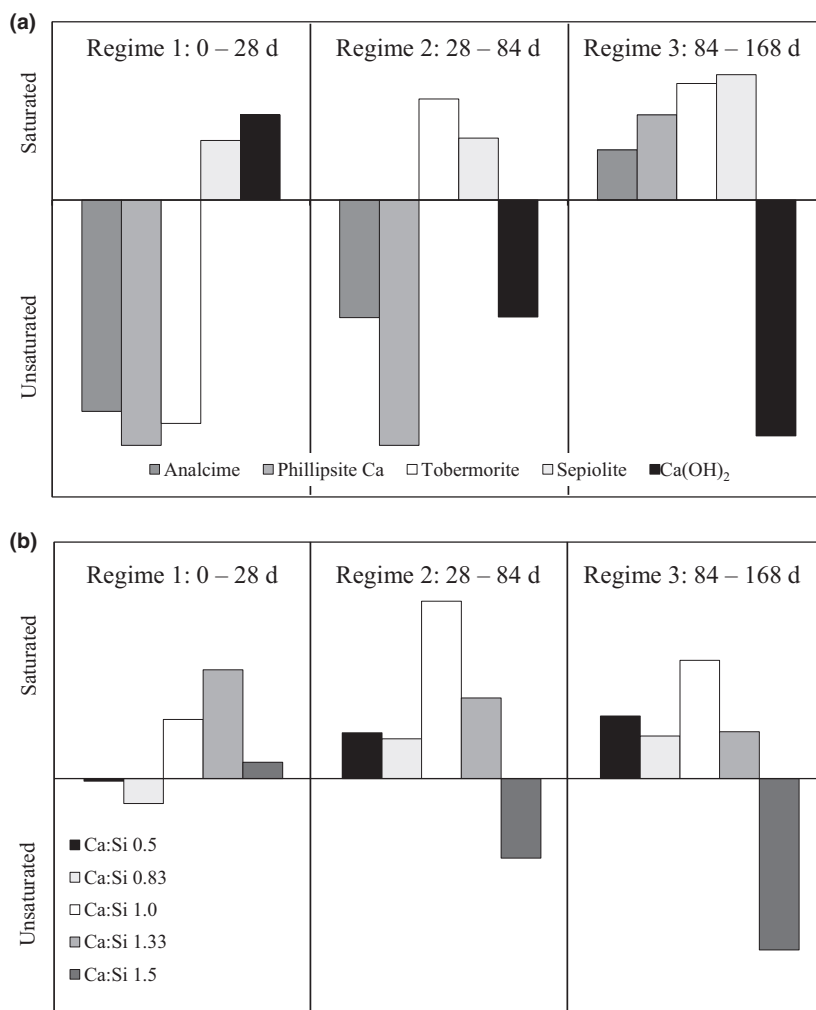


Fig. 2. (a) Saturation indices of selected species from the UK HLW glass powder dissolution in saturated $Ca(OH)_2$ solution during the three main phases of dissolution. Phases are: analcime ($Na_{0.96}Al_{0.96}Si_{2.04}O_6 \cdot H_2O$), phillipsite-Ca ($CaAl_2Si_5O_{14} \cdot 5H_2O$), tobermorite ($Ca_5Si_6(O, OH)_{18} \cdot 5H_2O$), sepiolite ($Mg_4Si_6O_{15}OH \cdot 6H_2O$), and $Ca(OH)_2$, and (b) relative saturation of Ca-silicate species in each main dissolution phase as a function of Ca:Si ratio, derived from the following PHREEQC species: 1.5 = jennite ($Ca_9Si_6O_{32} \cdot H_2O$), 1.33 = foshagite ($Ca_4Si_3O_9(OH)_2 \cdot 0.5H_2O$), 1 = xonotlite ($Ca_6Si_6O_{17}(OH)_2$), 0.83 = tobermorite (as above), and 0.5 = okenite ($CaSi_2O_4(OH)_2 \cdot H_2O$).

glasses¹⁸; phillipsite-Ca¹⁸ ($\text{CaAl}_2\text{Si}_5\text{O}_{14}\cdot 5\text{H}_2\text{O}$); sepiolite¹⁹ ($\text{Mg}_4\text{Si}_6\text{O}_{15}\text{OH}\cdot 6\text{H}_2\text{O}$); and tobermorite²⁰ ($\text{Ca}_5\text{Si}_6(\text{O},\text{OH})_{18}\cdot 5\text{H}_2\text{O}$). These phases are commonly referred to as silicate hydrates,²¹ which can incorporate Ca (C), Al (A), Na (N), and/or Mg (M) in a variety of combinations and wide range of compositions, for example Ca-Al-silicate hydrate or C-A-S-H. $\text{Ca}(\text{OH})_2$ saturation was also modeled.

Between 0 and 28 days, $\text{Ca}(\text{OH})_2$ was saturated in solution. The Mg-bearing silicate phase sepiolite was also saturated, indicating that it was thermodynamically possible for M-S-H phases to precipitate from solution during this time. All other phases were undersaturated, suggesting that C-(N)-A-S-H precipitation was not a major process governing the dissolution behavior during this phase. Between 28 and 84 days, $\text{Ca}(\text{OH})_2$ became undersaturated, concurrent with the Ca concentration decrease (Fig. 1f). In addition to sepiolite saturation, tobermorite became saturated, suggesting the likely precipitation of C-S-H phases during this dissolution regime. Between 84 and 168 days, C-(N)-A-S-H phases became saturated in solution (e.g. phillipsite-Ca and analcime). This behavior is indicative of Si saturation in solution. The changing composition of C-S-H phases with dissolution time can be expressed by the Ca-to-Si ratio in solution. Figure 2b shows that during the first phase of dissolution, only C-S-H phases with a Ca:Si ratio of >1 were likely to precipitate from solution (e.g. xonotolite, foshagite, and jennite). In the second and third phases of dissolution, C-S-H phases with a Ca:Si ratio of <1 were favored to precipitate (okenite, tobermorite, xonotolite, and foshagite), with the lower Ca:Si C-S-H species showing a greater propensity for saturation in the third phase of dissolution.

This change in C-S-H composition as a function of dissolution time is confirmed when the Ca and Si concentration data are plotted on a CaO-SiO₂-H₂O phase diagram,²² as shown in Fig. 3. At 21 and 28 days (at the beginning of the second regime of dissolution), the data plot on the C-S-H(I) metastable solubility curve, where C-S-H(I) corresponds to noncrystalline C-S-H phases with a Ca:Si ratio >1.5 . Between days 42 and 84, the data gradually shift towards the C-S-H(II) solubility curve, where C-S-H (II) corresponds to crystalline C-S-H phases with a Ca:Si ratio between 0.5 and 1. It is likely that solution compositions that plot between these fields would give rise to precipitates of C-S-H-(I). Data from day 140

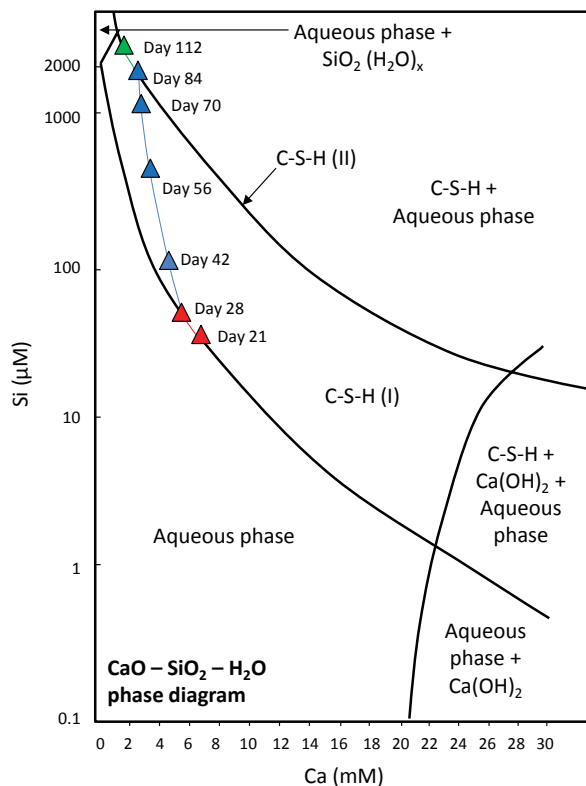


Fig. 3. Plot of Ca and Si solution concentrations from the dissolution of UK HLW glass powder in saturated $\text{Ca}(\text{OH})_2$ experimental solution at 50 °C on the CaO-SiO₂-H₂O phase diagram at 25 °C, adapted from Jennings (1986). Triangles show data points from the current study, from the initial detection of Si at day 21 to day 112 (further data points crowded the top of the chart). Coloured line shows trajectory of changing C-S-H composition in Regime 1 (red), Regime 2 (blue), and Regime 3 (green).

and 168 plot near the junction between the C-S-H + H₂O and SiO₂(H₂O)_x + H₂O stability fields (data not shown), suggesting that the solution was close to Si saturation. It should be noted that this diagram is relevant to the CaO-SiO₂-H₂O system at 25 °C, not at 50 °C as in the current study; therefore, Si saturation cannot be confirmed without further data.

UK HLW glass monolith dissolution in saturated $\text{Ca}(\text{OH})_2$

To investigate the dissolution of UK HLW glass at surface-area-to-volume ratios more relevant to the conditions likely to be encountered in a GDF, monolith samples with a surface-area-to-volume ratio of 10/m

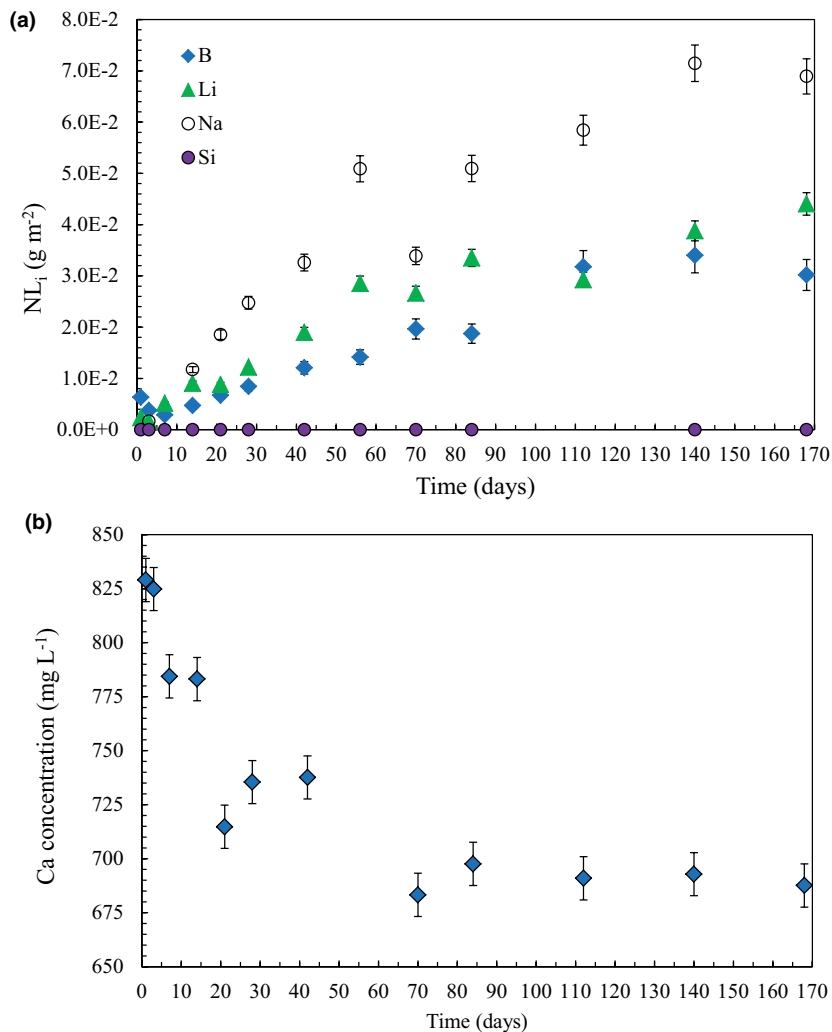


Fig. 4. (a) Normalized mass loss (g/m^2) of B, Li, Na, and Si as a function of time for UK HLW glass monoliths dissolved in saturated $Ca(OH)_2$ at $50^\circ C$ and (b) solution concentration (mg/L) of dissolved Ca in saturated $Ca(OH)_2$.

were used. The pH closely resembled that of the $Ca(OH)_2$ blank (Fig. 1a), which was approximately constant at $pH\ 12.5 \pm 0.3$ for the 168-day duration of the experiment. Only the soluble glass-forming elements, B, Li, and Na, were detectable in solution. The normalized mass loss of these elements was higher than for the powdered glass experiments (Fig. 4a, Table II), due to solution saturation effects in the powder experiments, resulting from the high surface-area-to-volume ratio. In contrast to the glass powder experiments, the dissolution of these elements was observed to proceed via a two-step process. Between 0 and 70 days, the dis-

solution rate was relatively rapid, as shown in Fig. 4a and Table III. The dissolution rates decreased and began to plateau after 70 days. It was not possible to detect Si in solution for the duration of the experiment. The concentration of Ca in the solution used in the monolith experiment was observed to decrease between 0 and 70 days from 830 mg/L to $\sim 680\ mg/L$, as shown in Fig. 4b. After 70 days, the Ca concentration was approximately constant at $690 \pm 5\ mg/L$. The dissolution rate change of the soluble glass elements (B, Li and Na) appeared to correlate with the rate change in Ca removal from solution.

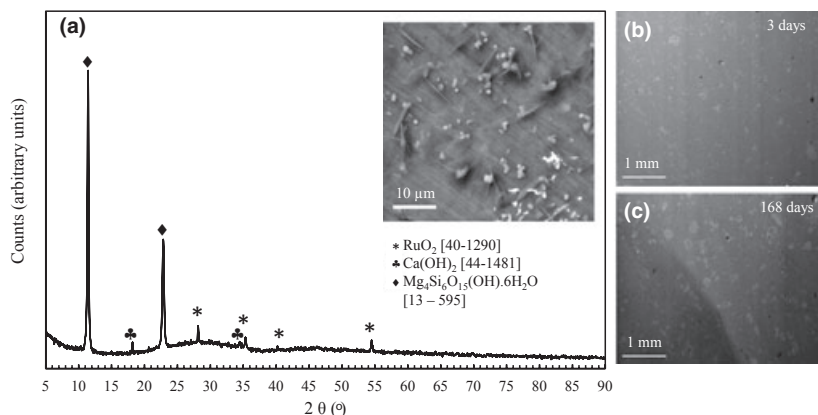


Fig. 5. (a) X-ray diffraction spectrum of surface precipitates observed on the surface of UK HLW glass monoliths after 3 days of dissolution in saturated $\text{Ca}(\text{OH})_2$ solution at 50°C . Spectrum was taken after 168 days of dissolution. Insert shows SEM images of large, amorphous surface precipitates after (b) 3 days and (c) 168 days of monolith glass dissolution.

Analysis of the monolith sample by powder XRD revealed the presence of an M-S-H phase (sepiolite $\text{Mg}_4\text{Si}_6\text{O}_{15}(\text{OH})_2 \cdot 6\text{H}_2\text{O}$, card 13–595) on the surface of the glass, which appeared after 3 days of dissolution (Fig. 5a). Also present at the surface were small ($\sim 10\ \mu\text{m}$) acicular crystallites and rounded particles $\sim 1\ \mu\text{m}$ in size (SEM inset, Fig. 5a). XRD and SEM/EDS analysis indicated that the rounded particles may be un-dissolved or precipitated $\text{Ca}(\text{OH})_2$; the acicular RuO_2 crystallites were present in the as-prepared glass. In addition, large areas ($>250\ \mu\text{m}$) comprised of a phase rich in Ca and Si, with no distinct crystalline texture, were observed after 3 days (Fig. 5b, EDS analysis not shown). After 168 days, the distribution of these phases was increased, and they had increased in size (up to $\sim 400\ \mu\text{m}$, Fig. 5c).

Figure 6 shows a back scatter electron (BSE) cross-section image of the glass monolith reacted for 168 days embedded in epoxy resin. Between the light (glass) and black (epoxy) areas, there is a two-component zone of material of intermediate BSE intensity. The first is $\sim 3\ \mu\text{m}$ in thickness immediately adjacent to the glass, rich in Si, which appears separated due to dehydration during drying of the sample. Immediately adjacent to the Si-rich layer, there is an area $\sim 60\ \mu\text{m}$ thick containing large precipitated phases. An EDS line scan taken across the second region of the altered zone indicated that where high intensities of Ca occurred, there were also increased intensities of Si, Mg, and Al, providing an indication that C-(A)-S-H and M-S-H phases may be forming a layer on the surface of the glass as a result of dissolution.

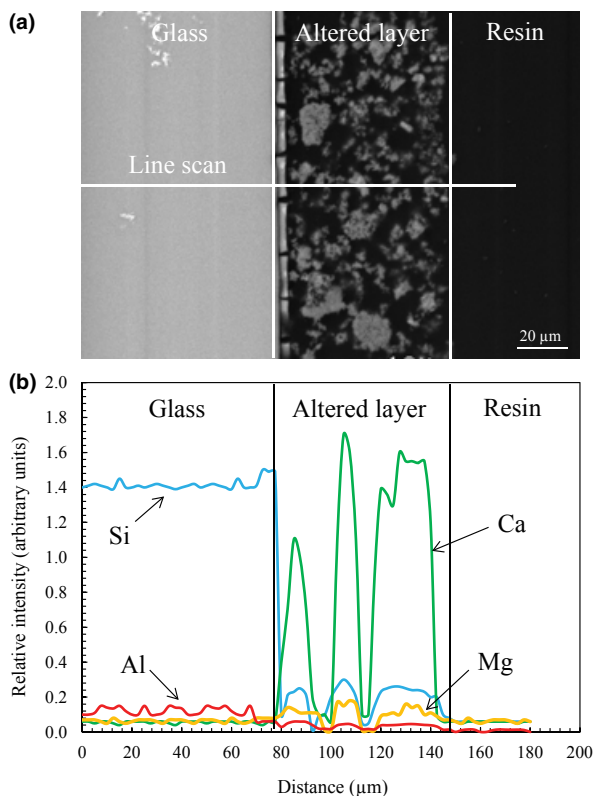


Fig. 6. (a) Backscatter electron image and (b) EDS line scans taken along the cross section of the UK HLW glass monolith surface after 168 days of dissolution in saturated $\text{Ca}(\text{OH})_2$ solution at 50°C showing the morphology and chemical composition of the Ca-, Si-, Al-, and Mg-rich altered layer.

Discussion

Glass alteration mechanism in the presence of water

Dissolution of high surface-area-to-volume ratio UK HLW glass powder in water indicated that dissolution proceeded with an initial fast rate, which progressively decreased with time. Between 0 to 28 days, Li and Na were released at a rapid rate, corresponding to well-known processes of interdiffusion (ion-exchange) and hydrolysis, replacing alkali ions in the glass by hydronium (H_3O^+). Dissolution was shown to be incongruent, due to the preferential release of Na over Li and B; Na and Li are loosely bound network modifiers, while B is a strong network former; hence, less energy may be required to break Na and Li bonds. Si was rapidly released during this time, reaching a maximum at 28 days.

A second regime was shown to occur between 28 and 168 days. During this regime, the dissolution rate of the glass, as determined by the release of B, Li, and Na, decreased by approximately one order of magnitude. In such a closed system, continuous ion exchange and hydrolysis can lead to increasing elemental concentrations with time, such that certain elements, particularly Si, reach solution saturation. When this occurs, glass network recondensation can be observed, where Si recondenses to form a gel layer on the surface of the glass. It has been suggested by others²³ that silica saturation is a prerequisite for this rate drop regime. The normalized mass loss data observed in this study show such a connection and indicate that when the normalized mass loss of silica in solution increases and becomes constant, the rate of glass dissolution decelerates, at 28 days. Without further analysis of the surface of the glass (precluded by the use of fine powders), we are not yet able to confirm the formation of an alteration layer; but based on the comparison of this behavior with other glass formulations (e.g. SON68¹⁸), we hypothesize that its formation is likely. The data in this study are consistent with a rate decrease mechanism involving either diffusion control from the protective alteration layer (i.e. kinetic effects) or solution saturation (i.e. thermodynamic effects). Although the surface area of glass used in these experiments was high (10 000/m), “quasi-equilibrium” was not observed after 168 days, however it appeared that the release of glass elements was approaching a residual rate by the end of the experiment. These data confirm that UK HLW MW+25% blend glass dissolution in

water proceeds *via* a general mechanism agreed widely in the literature¹⁸ and give the first insight into the long-term dissolution behavior of this glass. Further work is currently underway to ascertain the composition of a possible alteration layer and its effect on dissolution.

Glass Alteration in the Presence of Ca

This study provides the first detailed analysis of the durability of UK HLW glass under conditions potentially relevant to a colocated GDF. The experiments and data detailed here suggest that Ca in solution has a complex effect on the dissolution of UK HLW glass. Overall, the effect is to reduce the dissolution rate by an order of magnitude, compared with dissolution in water. Such effects seem remarkably different depending on the surface-area-to-volume ratio employed, and data suggest that they are intrinsically linked to the concentration of Ca in solution. This conclusion is in agreement with the recent work of several authors,^{7,9,10} including Mercado-Depierre *et al.*¹¹ who proposed that three key parameters control the behavior of glass dissolution in the presence of Ca: the pH, the surface-area-to-volume ratio (or whether long-term or short-term dissolution is being investigated), and the calcium concentration. It is clear from the results presented here that these parameters are key influences on dissolution; however, we propose that the primary control on glass dissolution in saturated $\text{Ca}(\text{OH})_2$ solution is equilibrium thermodynamics (or rather, in the case of glass, which cannot attain true equilibrium, quasi-equilibrium thermodynamics), which includes the solubility of the aqueous phase (dissolved Ca and Si) and the solid phase (C-S-H). This is discussed below with reference to three distinct regimes of dissolution that were identified during the dissolution of UK HLW powder in $\text{Ca}(\text{OH})_2$. These are summarized in Fig. 7 and are: i) the initial or incubation regime, from 0 to 28 days; ii) the intermediate regime, from 28 to 84 days; and iii) the “residual” regime, from 84 days until the end of the experiment at 168 days.

Initial “incubation” regime: Between 0 and 28 days, there was a rapid release of B, Li, Na, and Al into solution. This is concurrent with interdiffusion processes, resulting in an alkali-depleted, silicon-rich zone at the glass surface. Hydrolysis of the glass leads to the rupture of Si bridging bonds, leading to the release of orthosilicic acid, H_4SiO_4 , according to

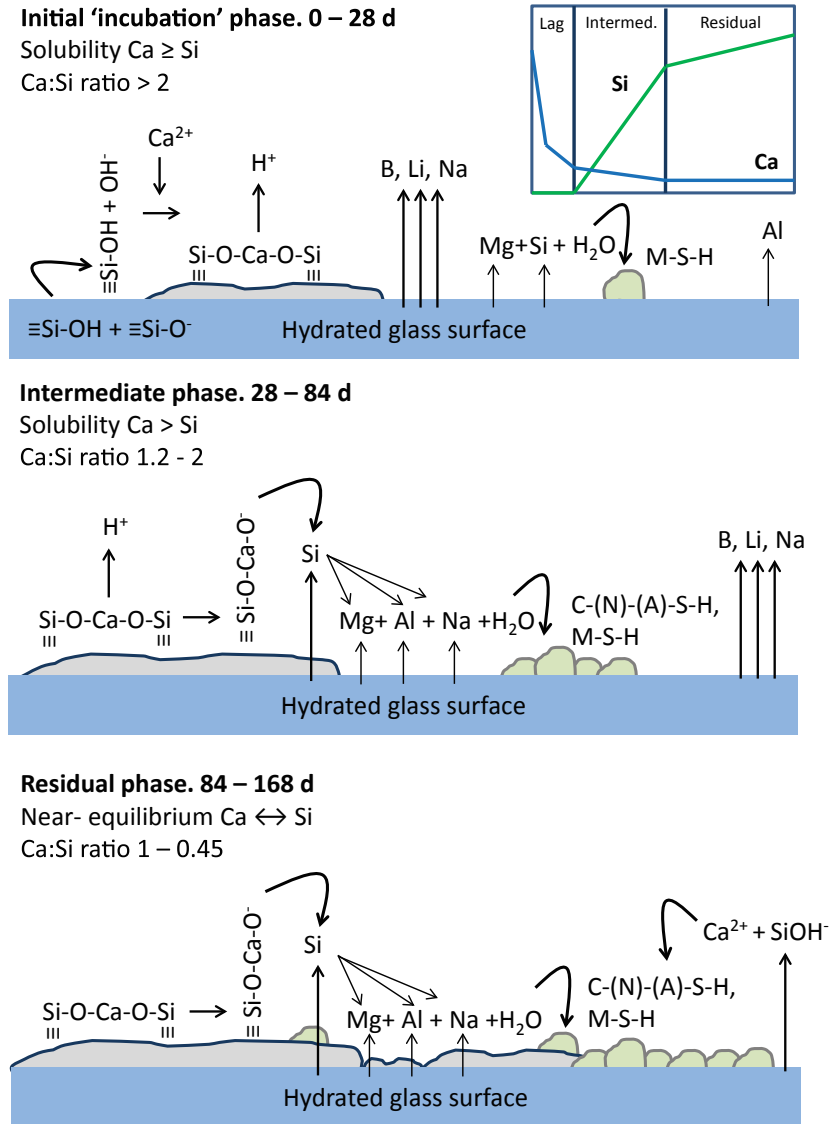
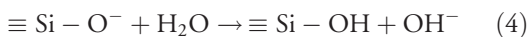
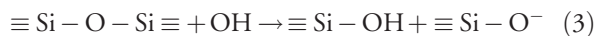


Fig. 7. Schematic diagram of hypothesized UK HLW glass powder dissolution in saturated Ca(OH)₂ solution, as a function of three main regimes of dissolution and Ca/Si solubility. Inset (top right) shows a schematic diagram of the normalized mass loss of Si and the solution concentration of Ca throughout the experiment.

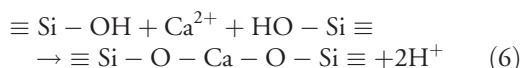


Geochemical modeling of the experimental solution indicated that M-S-H phases, formed from orthosilicic acid released during hydrolysis, may pre-

cipitate in the initial “incubation” regime, accounting for the retarded release of Si (hence the term “incubation regime”). The NL_(Mg) remained very low, suggesting that Mg concentration was controlled by the precipitation of secondary phases. Furthermore, XRD analysis of UK HLW glass monoliths found that a crystalline M-S-H phase was precipitated after 3 days of dissolution. This indicates that any Si released into solution during the initial dissolution

regime may react with dissolved ions, likely Mg in this experiment.

As a result of the initial release of orthosilicic acid (Eq. 3-5), the solution pH decreased. In the presence of Ca, a further decrease in the pH was concurrent with Ca consumption, as shown in Fig. 1a and f, and its incorporation within a hydrated amorphous silicate layer according to Eqn 6 is observed⁸ (Fig. 5b,c):



Hence, Ca reacts with silica at the surface, possibly through Ca-ion penetration to the hydrated glass, forming discrete patches of C-S-H. The accumulation of such phases does not seem to impede the release or diffusion of species into solution, at least up until 28 days. This is in agreement with Cailleteau *et al.*²⁴ who showed that the presence of Ca impedes the re-condensation of Si at the glass surface.

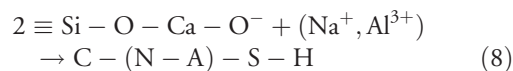
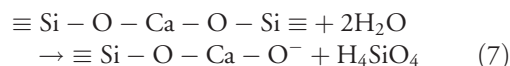
In the simplified system CaO-SiO₂-H₂O (Fig. 3), the concentrations of Si and Ca in the aqueous phase are coupled to the precipitation of C-S-H phases by equilibrium thermodynamics, such that when aqueous concentrations of Ca are high, those of Si are low and *vice versa*.²⁵ The glass must dissolve to maintain quasi-equilibrium conditions. As a result, Ca is absorbed into the altered glass surface and C-S-H is precipitated.²² In accordance with this thermodynamic analysis, during the first 28 days of dissolution in the current study, the solution was saturated with respect to Ca(OH)₂ (Fig. 2a). Interestingly, the NL_(Al) was observed to continuously increase in solution during this regime, suggesting that it is not thermodynamically favorable to form C-A-S-H over M-S-H in the presence of Ca under these conditions.

Intermediate regime: Between 28 and 84 days, the dissolution rate of glass, as indexed by the release of B, Li, and Na, continued but at a slower rate than during the initial regime (by a factor of 2 for B and Li, and a factor of 1.5 for Na). During this regime, the solution became undersaturated with respect to Ca(OH)₂ (Fig. 2a), Ca concentration decreased from ~200 mg/L at 28 days to ~80 mg/L (with a corresponding decrease in pH, Figs. 1a-f) and to maintain near-equilibrium conditions, Si was observed to rapidly dissolve into solution (Fig. 1e).

Previous thermodynamic investigations of the CaO-SiO₂-H₂O system have shown that Si release into

solution is restricted to Ca:Si ratios between 0.05 and 1.2²⁵, which correspond to solution concentrations of Ca between ~25 and ~100 mg/L. Similarly, in the current study, the release of Si to solution was observed when the solution concentration of Ca decreased below ~200 mg/L. Chave *et al.*⁸ investigated the effect of initial Ca concentration on the dissolution of a simplified French reference nuclear glass and found, in agreement with the above hypothesis, that a C-S-H alteration phase on the surface of the glass was only formed when Ca solution concentrations were less than 100 mg/L and that the thickness of the alteration layer increased with decreasing Ca concentration below this value, at 50 and 5 mg/L. Utton *et al.*⁹ also report the occurrence of an incubation regime in the dissolution of UK intermediate-level waste glass in Ca-saturated solution. This was observed between 0 and 7 days for experiments conducted at 90°C, and between 0 and 21 days for experiments at 50°C. In both instances, Si was not detected in solution until Ca concentrations were below 200 mg/L. The results presented here, and those of others, suggest that the release of significant quantities of Si only occur when the Ca:Si ratio in solution is within a tightly bound limit. Indeed, when the solution data for this regime are plotted on a CaO-SiO₂-H₂O stability diagram (Fig. 3), they fall in the stability field for C-S-H + Ca(OH)₂ + H₂O where phases with a Ca:Si ratio between 0.5 and 1.5 are expected to form, gradually becoming more Si-rich with time.

Because NL_(Si) was observed to rapidly increase in solution during this regime, it can be suggested that a passive reactive barrier to dissolution is not formed by the C-S-H phases. The rate decrease shown by B, Li, and Na is therefore likely to result from conditions approaching solution saturation, that is, approach to thermodynamic “quasi”-equilibrium. Because the RL_(Na) decreased more than for B and Li and the solution concentration of Al was shown to decrease (Fig. 1h), more complex silicate hydrates may form, involving Na and Al when Si is dissolved from the Ca-bridging species (Fig. 6):



Geochemical modeling suggested that during this dissolution period zeolitic C-(N)-A-S-H species

including mesolite ($\text{Na}_2\text{Ca}_2(\text{Al}_2\text{Si}_3\text{O}_{10})_3 \cdot 8\text{H}_2\text{O}$) and chabazite ($\text{CaAl}_2\text{Si}_4\text{O}_{12} \cdot 6\text{H}_2\text{O}$) became saturated in solution and thus may precipitate.

Residual regime: After 84 days, and until the end of the experiment at 168 days, the normalized dissolution rate of B, Li, and Na decreased further (by a factor of 2.5 for B and Li compared with the intermediate regime, and a factor of 3 for Na), and the $\text{RL}_{(\text{Si})}$ decreased by a factor of 1.6. This is concurrent with the onset of approximately constant pH (pH 10.5 ± 0.2) and Ca concentration ($\sim 65 \pm 10$ mg/L) conditions. The solution Ca and Si data plot on the C-S-H(II) metastable solubility line on the CaO-SiO₂-H₂O solubility diagram (Fig. 3). This line separates the stability fields of C-S-H + Ca(OH)₂ from C-S-H + H₂O, indicating that Ca (and hence Si) quasi-equilibrium is achieved. Geochemical modeling of the experimental solution shows that phases with a Ca:Si ratio < 1 are likely to form and shows there is an increasing propensity to form C-S-H phases with lower Ca:Si ratios (Fig. 2b). It is not clear whether C-S-H-type precipitates passivate the dissolution of elements from the glass surface in this regime or whether solution saturation is the controlling factor for the dissolution rate. Further work is required to elucidate this behaviour based upon the insight gained from geochemical modelling. Investigations are currently underway to fully identify the C-S-H phases that form during dissolution.

Surface Area to Volume Effects on Dissolution in the Presence of Ca

At low surface-area-to-volume ratios, such as those that occur when using a monolith sample, the dissolution behavior is different to that described above for high surface-area-to-volume ratios. The results described here suggest that dissolution occurs in a two-step process, with an initial regime between 0 and 70 days and an intermediate regime, between 70 and 168 days. Between 140 and 168 days, the $\text{NL}_{(\text{i})}$ of B, Li, and Na appear to become constant; however, further data are required to confirm whether the system reached steady-state dissolution. The two main regimes are marked by a change in the dissolution rate of B, Li, and Na, from high values in the initial regime to lower values in the intermediate regime (Fig. 4a, Table III), and also by a change in the Ca concentration (Fig. 4b). In the initial

regime, the Ca concentration decreased to 680 mg/L, and in the intermediate regime, it was constant at 690 ± 5 mg/L. For the duration of the experiment, the pH remained constant at pH 12.5 ± 0.3 . Notably, it was not possible to detect significant quantities of Si in solution (Fig. 4a).

Considering the hypothesis that the rate-limiting step of dissolution in Ca-rich solution is the equilibrium of Ca and Si, it is clear that in this system the solution is saturated with respect to Ca(OH)₂ for the duration of the experiment; thus, it is not thermodynamically favorable for Si to be released into solution. Accordingly, the main process likely to occur during this regime is the incorporation of Ca onto the hydrated glass surface (Eqn. 5), thus the dissolution is still in the initial “incubation” regime. The low surface-area-to-volume ratio results in fewer sites for Ca incorporation compared with high surface-area-to-volume ratios; thus, the Ca concentration becomes constant at high concentrations (680 mg/L, compared with 65 ± 10 mg/L for high SA/V), inhibiting dissolution of Si and formation of C-S-H phases. This may explain why Mercado-Depierre *et al.*¹¹ did not observe an incubation regime in their dissolution of glass in Ca-rich solution – a SA/V ratio of 20 000/m was utilized, such that Ca removal from solution occurred rapidly due to the higher number of accommodating surface sites, and thus, Ca–Si “quasi”-equilibrium was attained on more rapid timescales. It may be hypothesized that should this low surface-area-to-volume ratio system be given more time to react the same dissolution processes as observed for high surface-area-to-volume ratios may occur.

After 168 days of dissolution, a preliminary analysis of the alteration layer on the monolith surface was made. Patches of amorphous material containing Ca and Si were observed on the surface after 3 days, which increased in size by 168 days (Fig. 5b–c) but did not fully cover the surface. Precipitates of Mg-silicate were also identified, as were RuO₂ crystallites originally present in the glass.²⁶

Closer analysis of the alteration layer in cross section found that the thickness of this layer was ~ 60 μm , and contained large precipitates comprised of Ca, Si, Mg and Al, consistent with geochemical modelling analysis. It has been shown that the thickness of alteration layers resulting from glass dissolution in the presence of Ca increased in thickness with decreasing Ca concentration below 100 mg/L (maximum thickness of

~0.9 μm after 60 days of dissolution in solution Ca concentrations of 5 mg/L).⁸ It is interesting that the high Ca concentrations found in the current experiments lead to the formation of such a thick alteration layer. It is not clear whether this layer inhibits ion exchange between the glass and the solution, and although the dissolution rate of B, Li, and Na decreases with time, the effect of thermodynamic processes, that is, solution saturation, cannot be ruled out. To our knowledge, the current study and that of Chave *et al.*⁸ are unique in describing the formation of such an alteration layer in nuclear waste glasses; therefore, further work is underway to fully investigate this phenomenon.

Conclusion

The first detailed experiments on the dissolution of UK HLW MW+25 glass in Ca-saturated solution were conducted to understand the possible effects on glass alteration in a collocated geological disposal facility. Our findings suggest that dissolution in the presence of high concentrations of Ca (>200 mg/L) is an order of magnitude lower than dissolution in pure water. The rate-limiting step of dissolution of glass in Ca-rich solutions has been shown to be Ca-Si “quasi”-equilibrium, involving the precipitation of C-S-H phases. Considering the disposal of HLW glass in a collocated repository with a cementitious backfill, where the SA/V ratio will be very low, this suggests that dissolution is likely to be lower than a repository that does not use a Ca-rich backfill. However, it remains to be seen whether Si derived from cement backfill will adversely influence the dissolution of HLW glass. C-S-H phases in cement have been shown to strongly sorb radionuclide species,^{27,28} and it has been found that the Ca:Si ratio of these phases affect the extent of sorption. Further work is required to elucidate the C-S-H phases that form in these environments and in the alteration layer and their capacity for (i) inhibiting dissolution and (ii) incorporating radionuclide species from the glass.

This study demonstrates the complexity of potential interactions between glass and the hyperalkaline plume arising from the ILW zone of a collocated ILW/HLW geological disposal facility. Further work is required to fully elucidate the relevant glass alteration mechanisms to appraise the feasibility of such a collocated concept.

Acknowledgments

This work was funded in full by EPSRC under Grant EP/F055412/1: Decommissioning Immobilisation And Management of Nuclear Wastes for Disposal (DIAMOND). We are grateful to Dr. Paul Bingham and Prof. John Provis for useful discussions. CLC is grateful to the University of Sheffield for the award of a Vice Chancellor’s fellowship, and PGH would like to acknowledge the EPSRC Nuclear FiRST Doctoral Training Centre of the provision of a studentship under Grant EP/G037140/1. NCH is grateful to the Royal Academy of Engineering and the Nuclear Decommissioning Authority for funding. We are grateful to J. Icenhower (LLNL, USA) for insightful comments during review.

References

1. Geological Disposal: Steps Towards Implementation. Nuclear Decommissioning Authority report, NDA/RWMD/013, 2010.
2. Development of the Nirex Reference Vault Backfill; Report on Current Status in 1994. United Kingdom Nirex Ltd. Report number S/97/014, 1997.
3. Geological Disposal: Generic Environmental Safety Case Main Report. Nuclear Decommissioning Authority report, NDA/RWMD/021, 2010.
4. P. K. Abraitis, B. P. McGrail, D. P. Trivedi, F. R. Livens, and D. J. Vaughan, “Single-Pass Flow-Through Experiments on a Simulated Waste Glass in Alkaline Media at 40 °C: I. Experiments Conducted at Variable Solution Flow Rates to Glass Surface Area Ratio,” *J. Nucl. Mat.*, 280 196–205 (2000).
5. S. Gin and J. P. Mestre, “SON 68 Nuclear Glass Alteration Kinetics Between pH 7 and pH 11.5,” *J. Nucl. Mat.*, 295 83–96 (2001).
6. E. M. Pierce, W. E. A. Rodriguez, L. J. Calligan, W. J. Shaw, and B. P. McGrail, “An Experimental Study of the Dissolution Rates of Stimulated Aluminoborosilicate Waste Glasses as a Function of pH and Temperature Under Dilute Conditions,” *Appl. Geochem.*, 23 2559–2573 (2008).
7. Z. Andriambololona, N. Godon, and E. Vernaz, “Glass Alteration in the Presence of Mortar: Effect of the Cement Grade,” *Proc. Mat. Sci. Symp.*, 257 151–158 (1992).
8. T. Chave, P. Frugier, S. Gin, and A. Ayrat, “Glass-Water Interphase Reactivity with Calcium Rich Solutions,” *Geochim. Cosmochim. Acta*, 75 4125–4139 (2011).
9. C. A. Utton, R. J. Hand, P. A. Bingham, N. C. Hyatt, S. W. Swanton, and S. J. Williams, “Dissolution of Vitriified Wastes in a High-pH Calcium-Rich Solution,” *J. Nucl. Mat.*, 435 112–122 (2013).
10. C. A. Utton, R. J. Hand, N. C. Hyatt, S. W. Swanton, and S. J. Williams, “Formation of Alteration Products During Dissolution of Vitriified ILW in a High-pH Calcium-Rich Solution,” *J. Nucl. Mat.*, 442 33–45 (2013).
11. S. Mercardo-Depierre, F. Angell, F. Frizon, and S. Gin, “Antagonist Effects of Calcium on Borosilicate Glass Alteration,” *J. Nucl. Mat.*, 441 402–410 (2013).
12. C. A. Utton, S. W. Swanton, J. Schofield, R. J. Hand, A. Clacher, and N. C. Hyatt, “Chemical Durability of Vitriified Wasteforms: Effects of pH and Solution Composition,” *Min. Mag.*, 76 2919–2930 (2012).
13. E. Curti, L. Crovisier, J. L. Morvan, and A. M. Karpoff, “Long-term Corrosion of Two Nuclear Waste Reference Glasses (MW and SON68): A Kinetic and Mineral Alteration Study,” *Appl. Geochem.*, 21 1152–1168 (2006).

14. ASTM Standard Test Methods for Determining Chemical Durability of Nuclear, Hazardous, and Mixed Waste Glasses and Multiphase Glass Ceramics: The Product Consistency Test (PCT). *ASTM International* (2008). doi: 10.1520/C1285-02R08.
15. ASTM C 1220-98, Standard Test Method for Static Leaching of Monolithic Waste Forms for the Disposal of Radioactive Waste. *ASTM International* (2004).
16. D. L. Parkhurst, "User's Guide to PHREEQC – A Computer Program for Speciation, Reaction-Path, Advective Transport, and Inverse Geochemical Calculations," US. Geological Survey Water-Resources Investigations Report 95-4227, 143 (1995).
17. P. G. Heath, C. L. Corkhill, M. C. Stennett, R. J. Hand, W. C. H. M. Meyer, and N. C. Hyatt, "Encapsulation of TRISO Particle Fuel in Durable Soda-Lime-Silicate –Glasses," *J. Nucl. Mat.*, 436 139–149 (2013).
18. P. Frugier *et al.*, "SON68 Nuclear Glass Dissolution Kinetics: Current State of Knowledge and Basis of the New GRAAL Model," *J. Nucl. Mat.*, 380 8–21 (2008).
19. I. S. Muller, S. Ribet, I. L. Pegg, S. Gin, and P. Frugier, "Characterisation of Alteration Phases on HLW Glasses After 15 years of PCT Leaching," *Proc. Am. Ceram. Soc.*, 176 191 (2005).
20. B. Grambow and D. M. Strachan, "Leach Testing of Waste Glasses Under Near-Saturation Conditions," *Mat. Res. Soc. Symp. Proc.*, 26 623–634 (1984).
21. J. J. Chen, J. K. Thomas, H. F. W. Taylor, and H. M. Jennings, "Solubility and Structure of Calcium Silicate Hydrate," *Cement Concr. Res.*, 34 1499–1519 (2004).
22. H. M. Jennings, "Aqueous Solubility Relationships for Two Types of Calcium Silicate Hydrate," *J. Am. Ceram. Soc.*, 69 614–618 (1986).
23. S. Gin, "Protective Effect of the Alteration Gel: A Key Mechanism in the Long-Term Behaviour of Nuclear Waste Glass," *Proc. Mat. Res. Soc. Symp.*, 633 207–215 (2001).
24. C. Cailleteau *et al.*, "Insight into Silicate-Glass Corrosion Mechanisms," *Nat. Mater.*, 7 978–983 (2008).
25. U. R. Berner, "Evolution of Pore Water Chemistry During Degradation of Cement in a Radioactive Waste Repository Environment," *Waste Manag.*, 12 201–219 (1992).
26. P. Hrma, "Crystallisation During Processing of Nuclear Waste Glass," *J. Non-Cryst. Solids*, 356 3019–3025 (2010).
27. S. Aggarwal, M. J. Angus, and J. Ketchen, "Sorption of Radionuclides to Specific Mineral Phases Present in Repository Cements", AES Technology Report, AES-D&R-0395 (2000).
28. X. Gaona, E. Wieland, J. Tits, A. C. Sheinost, and R. Dahn, "Np(V/VI) Redox Chemistry in Cementitious Systems: XAFS Investigations on the Speciation Under Anoxic and Oxidising Conditions," *Appl. Geochem.*, 28 109–118 (2013).